Thermal conductivity and contact resistance of metal foams

E Sadeghi[1,2,3]**, S Hsieh**[2] **and M Bahrami**[2]

[1] Department of Mechanical Engineering, University of Victoria, Victoria, BC, V8W 3P6, Canada
[2] Mechatronic Systems Engineering, School of Engineering Science, Simon Fraser University, Surrey, BC, V3T 0A3, Canada

E-mail: ehsans@uvic.ca

Abstract

Accurate information on heat transfer and temperature distribution in metal foams is necessary for design and modelling of thermal-hydraulic systems incorporating metal foams. The analysis of heat transfer requires determination of the effective thermal conductivity as well as the thermal contact resistance (TCR) associated with the interface between the metal foam and the adjacent surfaces/layers. In this study, a test bed that allows the separation of effective thermal conductivity and TCR in metal foams is described. Measurements are performed in a vacuum under varying compressive loads using ERG Duocel aluminium foam samples with different porosities and pore densities. Also, a graphical method associated with a computer code is developed to demonstrate the distribution of contact spots and estimate the real contact area at the interface. Our results show that the porosity and the effective thermal conductivity remain unchanged with the variation of compression in the range 0–2 MPa; but TCR decreases significantly with pressure due to an increase in the real contact area at the interface. Moreover, the ratio of real to nominal contact area varies between 0 and 0.013, depending upon the compressive force, porosity, pore density and surface characteristics.

(Some figures in this article are in colour only in the electronic version)

1. Introduction

Transport phenomena in porous media have been the focus of many industrial and academic investigations [1–4]. The majority of the studies reported in the literature deal with low porosity media such as granular materials and packed beds [1, 2]. Over the last decade, high porosity microstructures such as open-cell metal foams have received more attention. Interest in these media stems from their relatively low cost, ultra-low density, high surface area to volume ratio and their ability to mix the passing fluid. These features are highly desirable for a wide variety of applications including microelectronics cooling, aerospace technology, filtration and compact heat exchangers [3–7]. In the majority of these applications, there is an interface between the foam and a solid surface which gives rise to an important phenomenon called thermal contact resistance (TCR) acting against heat transfer

in metal foams. Due to high porosity and irregularities of the free surface of metal foams, the actual contact area at the interface with a solid surface is very small; this emphasizes the significance of TCR at metal foam–solid surface interface. In some applications, metal foams are brazed to a metal sheet which may create a perfect contact, but because of high porosity of the medium, TCR still exists due to constriction and spreading of the heat flow passing through the metal sheet–foam interface.

A review of the literature indicates that in all previous studies related to heat transfer in metal foams, e.g. [8–15], the TCR was either neglected due to attachment of a metal sheet to the foam or 'bundled up' with the effective thermal conductivity and only the effective thermal conductivity value was reported. One fundamental issue with combining the two is that TCR is an *interfacial phenomenon* which is a function of mechanical load, surface characteristics and thermal conductivity of both interfacing surfaces, whereas thermal conductivity is a transport coefficient characterizing

---

[3] Author to whom any correspondence should be addressed.

the *bulk* medium. Thermal conductivity and TCR should therefore be distinguished. Furthermore, the effect of compression on thermal conductivity and TCR has not been thoroughly investigated.

The objective of this study is to measure the thermal conductivity and contact resistance of metal foams and estimate the size and distribution of contact spots (real contact area) at the interface. The experimental technique developed in this study allows the deconvolution of TCR and thermal conductivity and was used to perform a comprehensive experimental study to determine the effective thermal conductivity and TCR at different compressive loads.

A custom-made test bed was designed and built that enables the measurements of thermal conductivity and TCR of porous media under a vacuum. The test bed was equipped with a loading mechanism that allows the application of various compressive loads on the samples. ERG Duocel aluminium foams with various porosities and pore densities are used in the experiments. The tests are performed under a vacuum, where the test column was surrounded by an aluminium radiation shield to limit the radiation heat losses. The effective thermal conductivity and TCR are deduced from the total thermal resistance measurements by performing a series of experiments with aluminium foam samples of various thicknesses and similar micro-structures, i.e. porosity and pore density. Effects of compression, porosity and pore density are studied on the effective thermal conductivity and TCR.

To estimate the real contact area at the metal foam–solid interface, a pressure sensitive carbon paper is placed between the foam and the solid surface to print the contact spots at different compressive loads. A computer code is then developed using MATLAB to analyse the produced images and calculate the size of contact spots.

2. Thermal conductivity and TCR measurements

A schematic of the test bed for thermal measurements is shown in figure 1. The test chamber consists of a stainless-steel base plate and a bell jar enclosing the test column. The test column consists of, from top to bottom, the loading mechanism, the steel ball, the heater block, the upper fluxmeter, the sample, the lower fluxmeter, the heat sink (cold plate), the load cell and the polymethyl methacrylate (PMMA) layer. The heater block consists of circular flat copper in which a cylindrical pencil-type electrical heater is installed. The designed cold plate consists of a hollow copper cylinder, 1.9 cm high and 15 cm diameter. Cooling is accomplished using a closed loop water-glycol bath in which the coolant temperature can be set. The cold plate is connected to the chiller unit which adjusts the cold water temperature. A 1000 lbs load cell is used to measure the applied load to the sample. The fluxmeters were made of a standard electrolyte iron material. In this study, the cold plate temperature and the power of the electrical heater were set on 0 °C and 12 W, respectively.

To measure temperatures, six T-type thermocouples were attached to each fluxmeter at specific locations shown in figure 1. The thermocouples were located 5 mm apart with
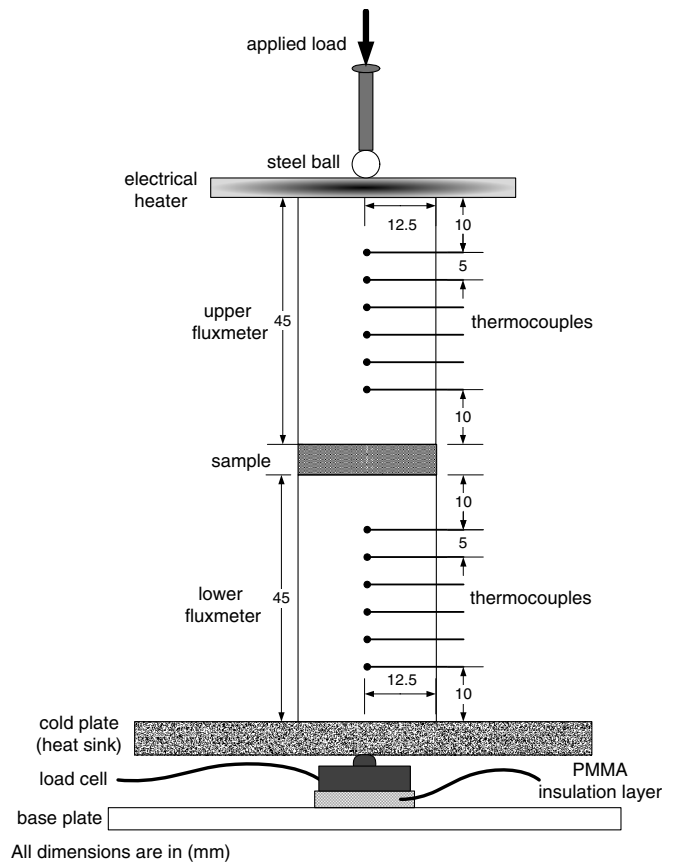
Figure 1. Schematic of the test bed for thermal measurement.

Table 1. Properties of the studied Al foam samples.

Sample number	#1	#2	#3	#4
Porosity	0.903	0.906	0.945	0.953
Pore density (PPI)	10	20	10	20
Thickness (mm)	13.93	13.90	13.92	13.93
	17.89	17.91	17.95	17.96

the first one 10 mm from the contact surface. The thermal conductivity of the iron fluxmeter was known and used to measure the heat flow rate transferred through the contact interface. The samples used in this study are open-cell aluminium foams. These Duocel foams were produced through a proprietary process developed by ERG in which the resulting foam has the identical chemical composition of the base alloy used. The foams were made of aluminium alloys of 6101 and cut in cylindrical shapes with the diameter of 25 mm and then were polished. Aluminium foam samples with the porosity range 90–96% and pore density of 10 and 20 PPI are used in this study; see table 1 for more details.

2.1. Test procedure

To study heat conduction only through the solid ligaments and contact surfaces, experiments were conducted under a vacuum. A vacuum level of 10^{-5} mbar was achieved under the test chamber using a vacuum machine. Temperatures and pressure were recorded at various compressive loads when steady-state conditions were achieved; to reach thermal

Table 2. Uncertainty of involving parameters in the analysis.

$\dfrac{\delta Q}{Q}$	$\dfrac{\delta \Delta T}{\Delta T}$	$\dfrac{\delta t}{t}$	$\dfrac{\delta A}{A}$	$\dfrac{\delta P_c}{P_c}$	$\dfrac{\delta \phi_s}{\phi_s}$
3.2%	1.7%	0.5%	0.8%	2.5%	2.2%

equilibrium all the experiment's parameters were kept constant and carefully monitored for approximately 4–5 h for each data point. The effects of compression were investigated over the range 0.3–2 MPa.

The temperature gradient between the hot and cold plates results in essentially one-dimensional heat transfer from the top to the bottom of the test column. Potential contribution of radiation heat transfer in the experimental setup can be divided into:

(1) Radiation inside the micro-structure: our measurements show that the maximum temperature difference between two neighbouring pores in the sample is 8.3 °C and temperature level inside the foam is less than 100 °C. After some calculations, we found that the contribution of radiation compared with conduction heat transfer inside the foam is less than 1%.

(2) Interfacial radiation: this radiation may occur between the fluxmeters and the metal foam surfaces at the interface. The temperature drops at the interface as a result of contact resistance. Our measurements show that this temperature drop is between 4 and 28 °C, depending on the compressive load. The maximum contribution of interfacial radiation compared with conduction is estimated to be less than 0.5%.

As a result, one can conclude the heat transfer in the present experiments is mostly due to conduction. The heat transfer through the fluxmeters can be determined using Fourier's equation:

$$Q = -kA \frac{\mathrm{d}T}{\mathrm{d}z}, \tag{1}$$

where $\mathrm{d}T/\mathrm{d}z$ is the temperature gradient along the test column, k is the thermal conductivity of the fluxmeters and A is the cross-sectional area of the samples/fluxmeters. The temperatures at the top and bottom contact surfaces can be extrapolated through the measured heat flux. The measured total thermal resistance at each pressure, R_{tot}, includes the sample (bulk) thermal resistance and the TCR (at the top and bottom interfaces) and can be expressed as

$$R_{tot} = R_{MF} + TCR = \frac{\Delta T_{ul}}{Q}, \tag{2}$$

where ΔT_{ul} is the temperature difference between the upper and the lower contact surfaces. R_{MF} and TCR are the metal foam resistance and the total contact resistance (summation of contact resistance at the top and bottom surfaces), respectively.

To deconvolute thermal conductivity and TCR, two experiments were performed with samples of different thicknesses; but with identical micro-structural parameters, e.g. porosity and pore density. Due to identical micro-structure and similar surface characteristics at the top and bottom interfaces, contact resistances for both samples can be considered equal at the same pressure. Applying equation (2)

to both measurements and subtracting them yields the effective thermal conductivity:

$$k_{eff} = \frac{t_1}{R_{MF1} A} = \frac{t_2}{R_{MF2} A}, \tag{3}$$

$$k_{eff} = \frac{t_1 - t_2}{(R_{tot1} - R_{tot2}) A}, \tag{4}$$

where t_1 and t_2 are the two different thicknesses of the Al foam sample at a specific applied pressure and A is the cross-sectional area of the sample. To investigate the effect of compression on the sample thickness, Al foam samples with different porosities ($0.9 < \varepsilon < 0.96$) and pore densities were compressed step by step using a standard tensile-compression machine. Thickness variation was measured for all samples at different pressures from 0 to 2 MPa using a Mitutoyo digital micrometer with the accuracy of 1 μm. The results show that the maximum thickness variation is less than 1.5% and may be neglected. Equation (4) can be used to find the effective thermal conductivity; the TCR can then be calculated by equation (2).

2.2. Uncertainty analysis

Considering the relationships for evaluating the effective thermal conductivity and the TCR, i.e. equations (4), (2), the relevant parameters in the analysis can be expressed as

$$R_{tot} = f(Q, \Delta T, t, A, P_c, \phi_s). \tag{5}$$

The main uncertainty in these experiments is due to errors in determining the heat flux through the sample which leads to a maximum error of 3.2%. The maximum uncertainties for the thermocouples and the data acquisition readings are ±1 °C which introduces a maximum error of 1.7% between the interfaces of the sample and the fluxmeters. The relative density of the similar samples with two different thicknesses was measured and the difference was used as a representative of the morphological uncertainty. This uncertainty as well as those associated with the load cell, thickness and cross-sectional area measurements are listed in table 2. The maximum uncertainty for the thermal resistance measurements can be calculated from [16]

$$\frac{\delta R_{tot}}{R_{tot}} = \left(\left(\frac{\delta Q}{Q} \right)^2 + \left(\frac{\delta \Delta T}{\Delta T} \right)^2 + \left(\frac{\delta t}{t} \right)^2 + \left(\frac{\delta A}{A} \right)^2 \right.$$
$$\left. + \left(\frac{\delta P_c}{P_c} \right)^2 + \left(\frac{\delta \phi_s}{\phi_s} \right)^2 \right)^{1/2}. \tag{6}$$

For this study, the maximum uncertainty is estimated to be ±5%.

3. Morphology of contact spots

To find the size and distribution of contact spots, a sheet of carbon copy paper along with a white paper was placed on the top and bottom of the samples. The assembly was compressed in a standard tensile-compression machine and the contact spots were printed on the white paper. The printed images were captured with a high resolution camera.

J. Phys. D: Appl. Phys. **44** (2011) 125406

E Sadeghi *et al*
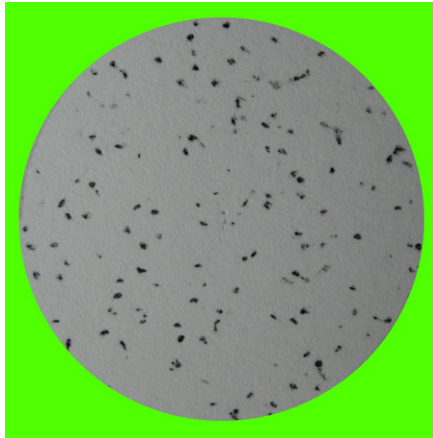
Figure 2. Masked image, Al foam with 95.3% porosity and 20 PPI at $P_c = 1.53$ MPa.
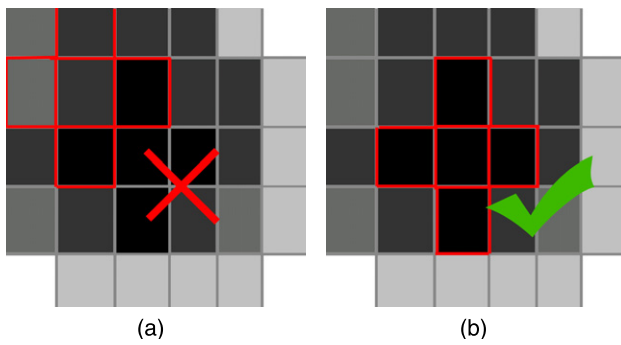

Figure 3. Contrast filtering.
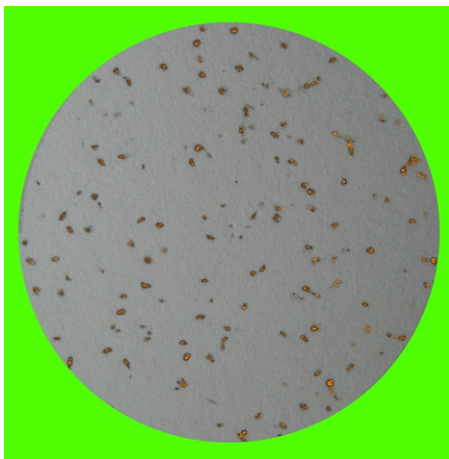
Figure 4. Highlighted contact points, Al foam with 95.3% porosity and 20 PPI at $P_c = 1.53$ MPa.

An image processing technique implemented in MATLAB enabled accurate evaluation of the contact area at the metal foam–solid interface. The image was first masked with green colour that highlighted the area of interest in a given RGB image shown in figure 2.

Analysing the green channel of the RGB image, the total pixel count/area of the sample can be found. Once the circular area of interest was found, the RGB image was converted into an 8-bit greyscale image where contact points can be extracted through image filtering by contrast. The contact points were
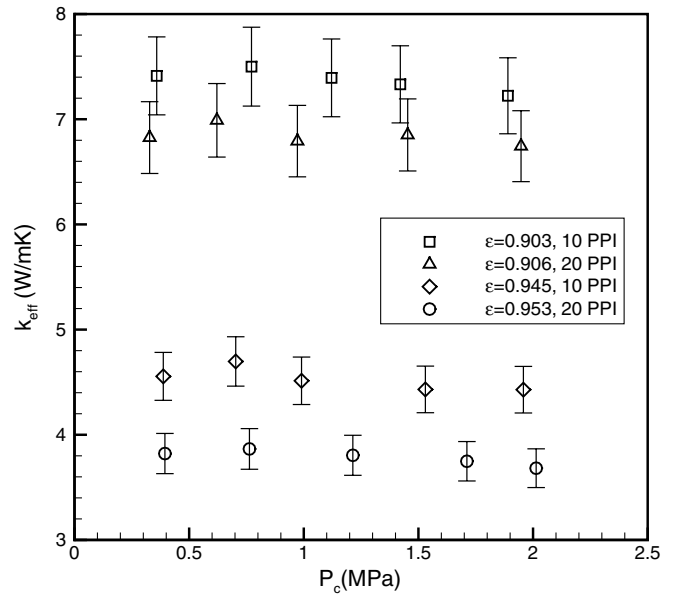
Figure 5. Effective thermal conductivity of different Al foam samples over a range of compression.
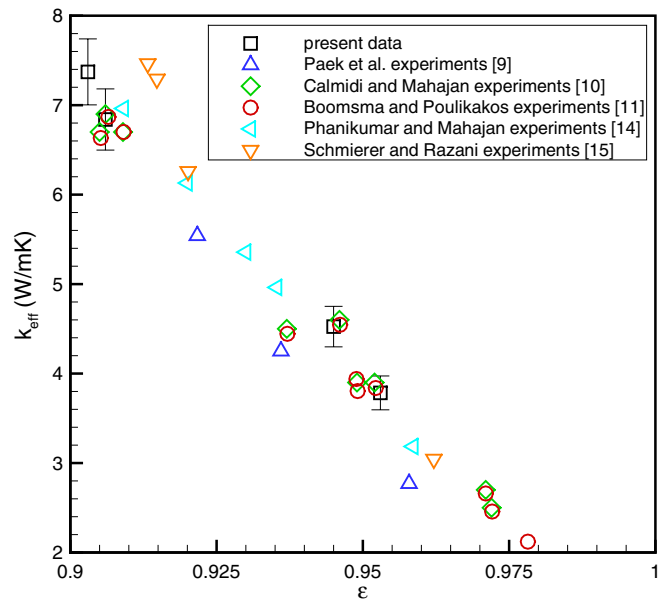
Figure 6. Present experimental data for Al foam-vacuum in comparison with existing experimental data for Al foam-air (data of [15] belongs to Al foam-vacuum experiments).
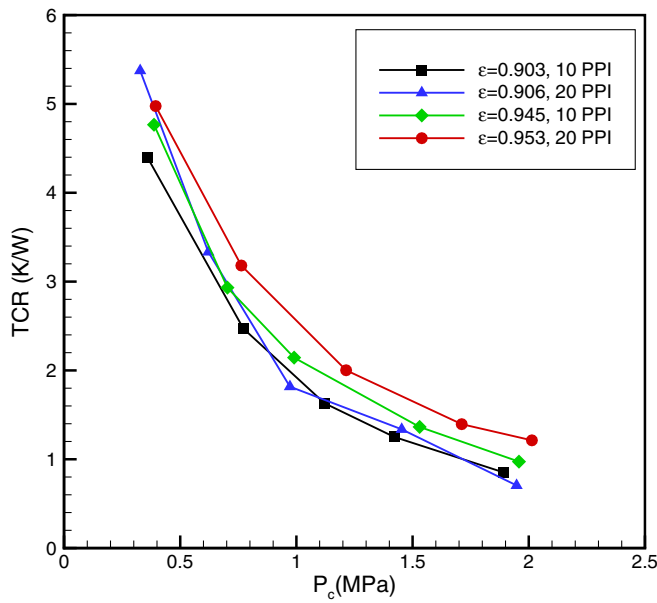
seen as dark spots in the image, where lighter shades of grey were shadows or blur caused by the camera. To differentiate contact spots and shadows, each pixel in the image was compared with their neighbouring pixels as seen in figure 3.

Each pixel was individually scanned in a cross pattern as seen in figure 3, the pixel in the centre of the cross was compared with the pixel directly above, below, left and right. The dark/lightness of the gradient was being monitored while contrast was being analysed simultaneously. The centre pixel in figure 3(*a*) appeared to be dark grey, and there is a change in its contrast to the surrounding pixels, hence, it is almost definite that this particular spot is a shadow and
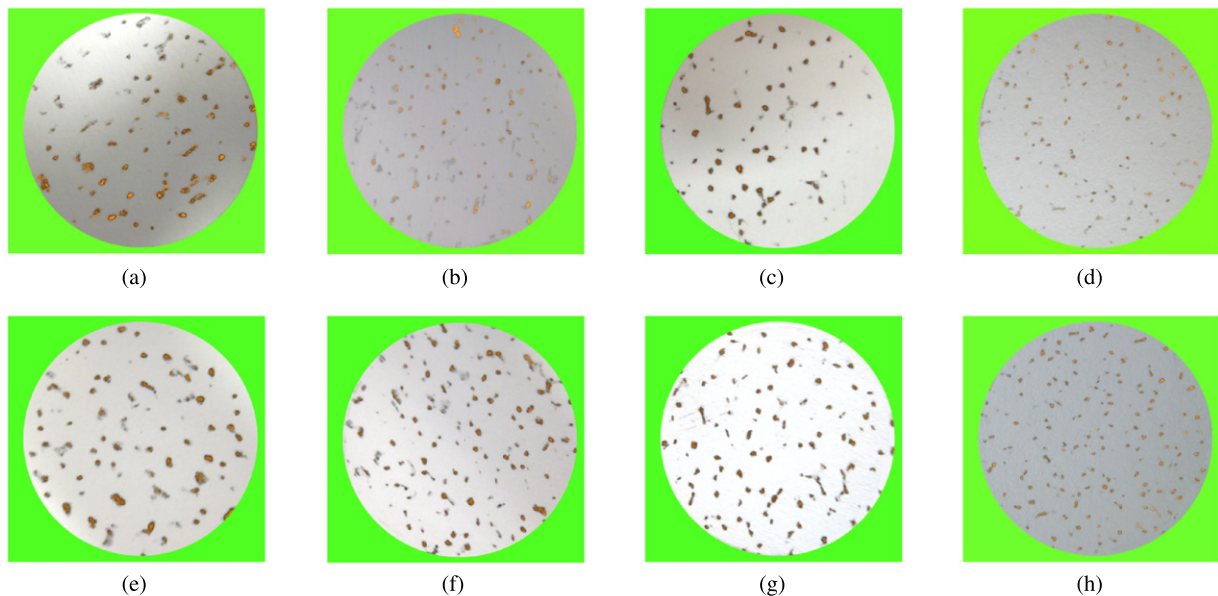
J. Phys. D: Appl. Phys. **44** (2011) 125406

E Sadeghi *et al*

not a contact point. However, in figure 3(*b*), the centre pixel met both requirements: (i) being dark compared with the background colour and (ii) negligible variation in contrast to the neighbouring pixels. Therefore, this location can be considered as a contact point. Each contact point was then highlighted with a different colour which is shown in figure 4.

Table 3. Averaged thermal conductivity of different samples over the compression range 0–2 MPa.

Sample number	#1	#2	#3	#4
k_{eff} (W m K^{-1})	7.37	6.84	4.53	3.78

Figure 7. TCR of different Al foam samples over a range of compression.

After scanning through the entire image, the pixel count of the contact spots were compared with the total area of the interface (circle shown in figure 4), and then the real contact area ratio was calculated.

4. Results and discussion

The measurements were taken at different compressive loads in a vacuum to study the effects of compressive load on TCR and effective thermal conductivity. Also, to find the real contact area at the metal foam–solid surface interface, separate compression tests were performed and the produced images were analysed using the developed image processing technique described in section 3.

Figure 5 shows the variation of the effective thermal conductivity with compression at different porosities and pore densities. The effective conductivity decreases with an increase in porosity; however, the effect of pore density seems to be insignificant. Lower porosity values are associated with a higher volume of solid ligaments which provide high conductive paths for the heat flow. Also, the effect of compressive load on the thermal conductivity is insignificant over the studies' pressure range. Our measurements show that the highest bulk deformation occurring under the compression is 1.5% which does not have a significant impact on the micro-structure. However, higher compressive loads, which produce larger deformations, may affect the thermal conductivity as reported in [4]. Table 3 summarizes the averaged effective thermal conductivity values of the metal foam samples measured in this study.

Present experimental data is compared with existing experimental data in figure 6. The majority of existing data [9–11, 14] were reported for Al foam-air; but since the thermal conductivity of air is very low, its contribution to the effective

Figure 8. Highlighted contact points for various Al foam samples: (*a*) $\varepsilon = 90.3\%$, 10 PPI at $P_{\mathrm{c}} = 1.43$ MPa; (*b*) $\varepsilon = 90.6\%$, 20 PPI at $P_{\mathrm{c}} = 1.02$ MPa; (*c*) $\varepsilon = 94.5\%$, 10 PPI at $P_{\mathrm{c}} = 1.32$ MPa; (*d*) $\varepsilon = 95.3\%$, 20 PPI at $P_{\mathrm{c}} = 1.02$ MPa; (*e*) $\varepsilon = 90.3\%$, 10 PPI at $P_{\mathrm{c}} = 2.85$ MPa; (*f*) $\varepsilon = 90.6\%$, 20 PPI at $P_{\mathrm{c}} = 2.44$ MPa; (*g*) $\varepsilon = 94.5\%$, 10 PPI at $P_{\mathrm{c}} = 3.06$ MPa; (*h*) $\varepsilon = 95.3\%$, 20 PPI at $P_{\mathrm{c}} = 3.06$ MPa.

thermal conductivity may be negligible. The compressive load for the existing experimental data was not reported; therefore, the mean values of the present data at different compressive loads are used for comparison purposes. As shown, the present experimental data agrees with the majority of existing data at different porosities; however, the data values reported by Paek *et al* [9] are lower compared to the other data. It should be noted that the TCR for the data collected from other sources [9–11, 14] is negligible since the foam samples were brazed to Al sheets, and the temperatures of the Al sheets near the contact points were used for evaluating thermal conductivity. Using the present and collected data, the following correlation is proposed for the effective thermal conductivity of Al foams:

$$k_{eff} = 67.7 - 67\varepsilon : 0.9 < \varepsilon < 1. \tag{7}$$

This equation correlates very satisfactorily (within 3%) with the present experimental data; however, all collected data agree with this correlation within 10%.

Figure 7 shows the variation of the TCR for the examined Al foam samples at different compressive loads. It can be seen that the compressive load has a pronounced effect on TCR. In addition, TCR is more sensitive to porosity rather than pore density. The real contact area at the foam–solid interface increases with an increase in the compressive load which results in a considerable reduction in TCR. Also, as expected, samples with higher porosities have lower solid material in the contact region which results in a higher TCR. Furthermore, the number of contact spots increases with an increase in pore density; however, these contact spots have a smaller size and a different surface profile. As a result of these competing effects, the effect of pore density on contact resistance is not significant.

Distribution of contact spots for different Al foam samples is shown in figures 8(*a*)–(*d*) for a moderate pressure and figures 8(*e*)–(*h*) for a high pressure. As shown, the total contact area decreases with an increase in porosity. Also, higher pore densities provide a larger number of contact points which can reduce the TCR as shown in figure 7. The real contact area and its ratio to nominal contact area, η, were found from the analysis of the printed images and are shown in figure 9. The nominal contact area was considered equal to the cross-sectional area, and η is defined as

$$\eta = \frac{\text{summation of area of contact spots}}{\text{metal foam cross-sectional area}}. \tag{8}$$

There is a small difference between the contact area ratio of the bottom and top surfaces due to different distribution of ligaments on these surfaces, therefore, in our analysis the averaged value of the contact area ratio for these surfaces is considered.

Reviewing figures 7–9 shows that for a relatively high pressure, the number and total area of contact spots increase with an increase in pore density and foam density which reduces the TCR. However, in low contact pressures, $P_c <$ 0.3 MPa, the contact surface morphology becomes more important and dominates the effects of pore density and porosity. Therefore, the smaller contact area (higher TCR) of denser foams such as the foam with $\varepsilon = 0.906$ can be due to a higher surface roughness.
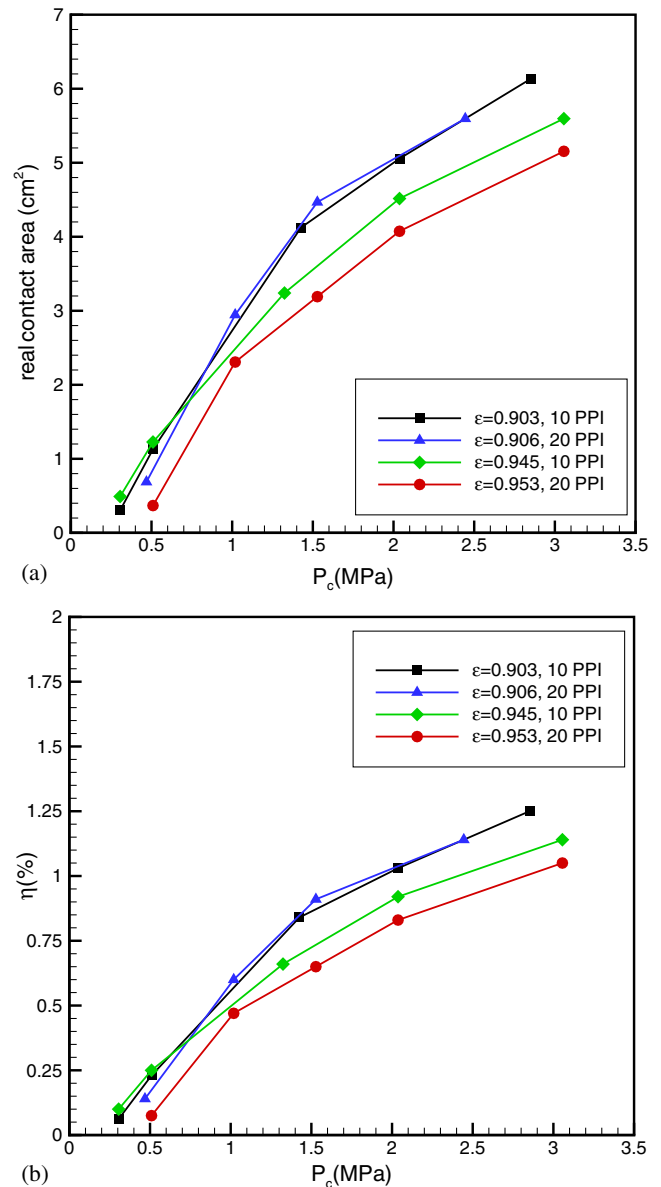

Figure 9. (*a*) Real contact area and (*b*) ratio of total contact area to cross-sectional area for various Al foam samples under compression.

Figure 10 shows the TCR to total thermal resistance ratio for examined Al foam samples with the average thickness of 13.92 mm at different compressive loads. As can be seen, TCR is the dominant resistance at low compressive loads, $P_c < 0.3$ MPa, constituting more than 50% of the total resistance. This contribution decreases for all samples with an increase in the compressive load. It is very interesting to observe that although the absolute value of TCR increases with an increase in porosity, its ratio to the total resistance decreases. This is due to the fact that both foam bulk resistance and TCR increase with porosity, but this increase is higher for the bulk resistance.

5. Summary and conclusions

A test bed was designed and built to measure the thermal conductivity and TCR of metal foams under various
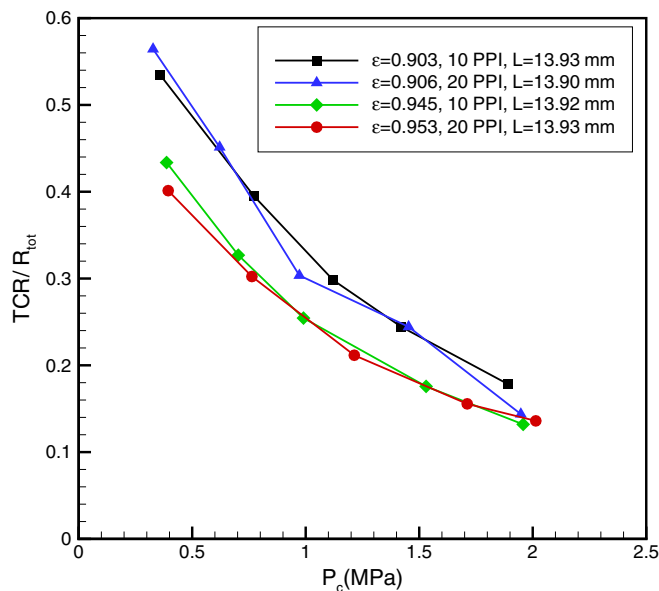
Figure 10. TCR to total thermal resistance ratio for different Al foam samples under compression.

compressive loads. Also, a computer program associated with an experimental setup was developed to find the distribution and total size of actual contact area at the metal foam–solid surface interface. The analytical modelling of thermal conductivity and TCR will be provided in a companion paper. The present experimental data for the effective thermal conductivity is in good agreement with existing data over a range of porosities. Our results show that the effective thermal conductivity increases with an increase in the foam density, but it is relatively insensitive to compressive load in the range 0–2 MPa.

An important finding is the large contribution of TCR to the total thermal resistance, more than 50%, for relatively low compressive loads. The high values of TCR are related to very small ratios of contact area to the cross-sectional area; the maximum ratio is 1.3% at the contact pressure of 3 MPa. TCR is more sensitive to the compressive load rather than porosity and pore density; however, it decreases with an increase in the foam density.

This work provided new insights on the importance of TCR and has helped to clarify the impact of this key interfacial phenomenon on the thermal analysis of metal foams.

Acknowledgments

References

[1] Kaviany M 1995 *Principles of Heat Transfer in Porous Media* (New York: Springer)
[2] Bahrami M, Yovanovich M M and Culham J R 2006 Effective thermal conductivity of rough spherical packed beds *Int. J. Heat Mass Transfer* **49** 3691–701
[3] Dukhan N, Picon-Feliciano R and Alvarez-Hernandez A R 2006 Heat transfer analysis in metal foams with low conductivity fluids *J. Heat Transfer* **128** 784–92
[4] Ozmat B, Leyda B and Benson B 2004 Thermal applications of open-cell metal foams *Mater. Manuf. Process.* **19** 839–62
[5] Bhattacharya A, Calmidi V V and Mahajan R L 2002 Thermophysical properties of high porosity metal foams *Int. J. Heat Mass Transfer* **45** 1017–103
[6] Hunt M L and Tien C L 1988 Effects of thermal dispersion on forced convection in fibrous media *Int. J. Heat Mass Transfer* **31** 301–9
[7] Mahjoob S and Vafai K 2008 A synthesis of fluid and thermal transport models for metal foam heat exchangers *Int. J. Heat Mass Transfer* **51** 3701–11
[8] Zhao C Y, Lu T J, Hodson H P and Jackson J D 2004 The temperature dependence of effective thermal conductivity of open-celled steel alloy foams *Mater. Sci. Eng.* A **367** 123–31
[9] Paek J W, Kang B H, Kim S Y and Hyun J M 2000 Effective thermal conductivity and permeability of aluminum foam materials *Int. J. Thermophys.* **21** 453–64
[10] Calmidi V V and Mahajan R L 1999 The effective thermal conductivity of high porosity fibrous metal foams *J. Heat Transfer* **121** 466–71
[11] Boomsma K and Poulikakos D 2001 On the effective thermal conductivity of a three-dimensionally structured fluid-saturated metal foam *Int. J. Heat Mass Transfer* **44** 827–36
[12] Krishnan S, Garimella S and Murthy J Y 2008 Simulation of thermal transport in open-cell metal foams: effects of periodic unit-cell structure *J. Heat Transfer* **130** 024503-024507
[13] Babcsan N, Meszaros I and Heman N 2003 Thermal and electrical conductivity measurements on aluminum foams *Materialwiss. Werkstofftech* **34** 391–4
[14] Phanikumar M S and Mahajan M L 2002 Non-darcy natural convection in high porosity metal foams *Int. J. Heat Mass Transfer* **45** 3781–93
[15] Schmierer E N and Razani A 2006 Self-consistent open-celled metal foam model for thermal applications *J. Heat Transfer* **128** 1194–203
[16] Taylor J R 1997 *An Introduction to Error Analysis: The Study of Uncertainties in Physical Measurements* (Sausalito, CA: University Science Books)